Table 2 Comparison of nonlinear coefficient $\bar{A}_2$ with the previous results for isotropic material

Geometry of the plate	Inplane boundary conditions: Constrained type I	Constrained type II	Unconstrained	Average of B.C. in column 3	Reference[a]
	...	3.9771	1.6130	1.8027	9
Rectangle,	...	6.0959	2.1792	...	8
Clamped	3.5771	3.5138	1.1582	...	Present
Rectangle,	...	2.9353	0.3952	0.7610	2,9 and 7
freely	...	...	0.1903	...	7
supported	...	2.9730	0.4648	...	8
	2.9830	2.9694	0.3829	...	Present

[a] All other results except the present ones are based on trigonometric modes for w.

equations, which were seen to be the two bounds for the exact value of A_2 for a given w. Such a bounding property has already been reported.[3] Typical numerical values of the nonlinear coefficient A_2 for various cases considered in Sec. II are given in Table 1 for $a/b=1$. These values are decomposed into two parts for the case of dynamic analog of the von Karman equations as discussed earlier. The accuracies of the various solutions obtained are also summarized in Table 1. The Galerkin approximations to the solutions of the inplane compatibility equation converged from below as expected. The Young's moduli for the orthotropic material are $E_1=28\times10^5$ kg/cm^2 and $E_2=2.24\times10^5$ kg/cm^2; the Poisson's ratios are $\nu_1=0.2$ and $\nu_2=0.016$; the shear modulus is $G_{12}=2.24\times10^5$ kg/cm^2. The properties of the isotropic material are $E_1=1\times10^5$ kg/cm^2 and $\nu_1=0.3$.

IV. Discussion

The values of A_2 in Table 1 clearly show the significant role played by the stretching due to the inplane displacements (i.e., uv stretching). Also, it is seen that in the case of plates with unconstrained boundary conditons, the inplane displacements introduce a predominantly compressive strain field, thus yielding a negative value for the uv stretching. It is conjectured that a re-examination of the Berger approximation to the nonlinear plate equations, with the role of uv and w stretching components being duly identified, might yield some interesting results. An extensive computation for a few aspect ratios revealed that the first-order Galerkin approximations to the solutions of the inplane equilibrium equations may yield a small uv stretching contribution in many cases, even though the accurate solutions yielded significant uv stretching components. Hence, Bert's[5] assumption of neglecting the uv stretching is not justified.

Considering the results in Table 2, it is seen that for the two types of constrained boundary conditions for a rectangular plate, the values of A_2 given by the present analysis do not differ appreciably. Similar observations were made by Dowell and Ventres[7] also. The present results for the constrained clamped rectangular plates are better than the previous results, because the polynomial mode for w is less stiff than the trigonometric mode used by others.

Considering the case of plates with edges free of inplane stress resultants (unconstrained), all other results in Table 2 (except the present results) are, in general, based on less accurate solutions to the inplane compatibility equations. However, the deviations between the present and previous results are both due to the aforementioned error and the different type of mode used for w. It has been observed that the first-order Galerkin approximations can have substantial error in the case of plates with unconstrained boundary conditions also. Although an averaged condition for the case of the unconstrained boundary condition has not been considered in the present analysis, the results in Table 2 clearly show the possible wide difference between these two conditions as observed by Dowell and Ventres;[7] only a one-term Galerkin approximation was obtained however. Finally, a comparison of the results due to Bayeles et al.[8] with various other results clearly shows the inadequacy of a first-order Galerkin approximation to the solution of the inplane equilibrium equations or the compatibility equation.

References

[1] Herrmann, G., "Influence of Large Amplitudes on Flexural Motions of Elastic Plates," TN 3578, 1955, NACA.

[2] Chu, H. N. and Herrmann, G., "Influence of Large Amplitudes on Free Flexural Vibrations of Rectangular Elastic Plates," *Journal of Applied Mechanics*, Vol. 23, 1956, pp. 532-540.

[3] Vendhan, C. P. and Das, Y. C., "Application of Rayleigh-Ritz and Galerkin Methods to Nonlinear Vibration of Plates," *Journal of Sound and Vibration*, Vol. 39, March 1975, pp. 147-157.

[4] Vendhan, C. P. and Dhoopar, B. L., "Nonlinear Vibration of Orthotropic Triangular Plates," *AIAA Journal*, Vol. 11, May 1973, pp. 704-709.

[5] Bert, C. W., "Nonlinear Vibration of a Rectangular Plate Arbitrarily Laminated of Anisotropic Material," *Journal of Applied Mechanics*, Vol. 40, June 1973, pp. 452-458.

[6] Leissa, A. W., "Vibration of Plates," SP-160, Ch. 7, 1969, NASA.

[7] Dowell, E. H. and Ventres, C. S., "Modal Equations for the Nonlinear Flexural Vibrations of a Cyclindrical Shell," *International Journal of Solids and Structures*, Vol. 4, Oct. 1968, pp. 975-991.

[8] Bayles, D. J., Lowery, R. L., and Boyd, D., "A Nonlinear Dynamic Lumped Parameter Model of a Rectangular Plate," *Journal of Sound and Vibration*, Vol. 21, April 1972, pp. 329-337.

[9] Yamaki, N., "Influence of Large Amplitudes on Flexural Vibrations of Elastic Plates," *Zeitschrift fur Angewandte Mathematik und Mechanik*, Vol. 41, 1961, pp. 501-510.

Approximate Shock-Free Transonic Solution for Lifting Airfoils

Sunil Kumar Chakrabartty*
Jadavpur University, Calcutta, India

Introduction

PRACTICAL and mathematical interests in transonic potential flow problems have grown in recent times through works of Nieuwland[4] and his co-workers in NLR, The Netherlands, and the experimental works of Holder and Pearcy[5] in England. Among the various analytical methods based on transonic small perturbation theory for studying transonic profile flow problem, the integral equation method of Oswatitsch, improved and extended further by Gullstrand, Spreiter, and Alksne,[2] is well known.

Nörstrud[6] extended the integral equation method of Oswatitsch to lifting flows by the finite difference method. Recently, Subramanian and Balakrisnan[7] extended the technique of local linearization method to lifting airfoils.

The present Note gives an extension of the simple approximate shock-free transonic solution of the integral equation of Oswatitsch given by Niyogi and Mitra[8] to the lifting case. Numerical results for parabolic arc profiles and the NACA 0012 profile at different angles of attack have been compared with previous analytical, numerical, and experimental results.

Basic Equations and Solution

Consider a steady, inviscid, non-heat-conducting, plane

Received August 12, 1974; revision received March 13, 1975. The author takes this opportunity to thank P. Niyogi, Reader in Mathematics, Jadavpur University, Calcutta for his kind help and continuous guidance in preparing this Note.

Index category: Subsonic and Transonic Flow.

*Research Scholar.

transonic, supercritical flow past a thin-cambered lifting airfoil under small perturbation, with freestream Mach number $M_\infty < 1$. The gas dynamic equation and the irrotationality condition can be converted into the following two-dimensional integral equation by the application of Green's theorem of potential theory[2,6]

$$\Phi(x,y) = \Phi_p(x,y) - \frac{1}{2\pi}\int_{-\infty}^{\infty}\int_{-\infty}^{\infty} \Phi_\xi \Phi_{\xi\xi} \ln\frac{1}{R}\, d\xi\, d\eta \quad (1)$$

Here $\Phi(X,Y)$ is the reduced velocity potential, and X, Y the reduced coordinates related to the true values, indicated by lower case letters, by the relations

$$\Phi(X,Y) = k(\varphi - u_\infty x - v_\infty)/[(1-M_\infty^2)u_\infty] \quad (2)$$

with X, Y as new independent variables defined by

$$x = \chi \qquad Y = (1-M_\infty^2)^{1/2} y \quad (3)$$

and k is a selective function of the freestream flow condition identified by the subscript ∞, and taken here to be

$$k = (1-M_\infty^2)^{1/2}/(M_\infty^{*-1} - 1)$$

$$R = [(x-\xi)^2 + (Y-\eta)^2]^{1/2} \quad (4)$$

where a body-fixed rectangular Cartesian coordinate system has been chosen, such that the X-axis coincides with the freestream direction. Φ_p denotes the corresponding linearized solution in reduced coordinates being defined by Eqs. (17) and (18).

Splitting up the solution of Eq. (1) into a symmetric part denoted by the superscript "+", and an antisymmetric part denoted by a superscript "—", and equating symmetric and antisymmetric parts on both sides as in the work of Nörstrud,[9] we obtain in the limit $Y \to 0$

$$\Phi_X^+(x,0) = [\Phi_p^+(X,0)]_X$$

$$- \frac{1}{2\pi}\int_{-\infty}^{\infty}\int_{-\infty}^{\infty} [\Phi_\xi^+ \Phi_{\xi\xi}^+ + \Phi_\xi^- \Phi_{\xi\xi}^-] \frac{\partial}{\partial\xi} ln\frac{1}{R}\, d\xi d\eta \quad (5a)$$

$$\Phi_Y^+(X,0) = [\Phi_p^+(X,0)]_Y \quad (5b)$$

$$\Phi_X^-(X,0) = [\Phi_p^-(X,0)]_X \quad (6)$$

$$\Phi_Y^-(X,0) = [\Phi_p^-(X,0)]_Y$$

$$- \frac{1}{2\pi}\int_{-\infty}^{\infty}\int_{-\infty}^{\infty} [\Phi_\xi^+ \Phi_{\xi\xi}^- + \Phi_\xi^- \Phi_{\xi\xi}^+] \frac{\partial}{\partial\eta} \ln\frac{1}{R}\, d\xi d\eta \quad (7)$$

where the suffixes X and Y denote differentiation.

For a symmetric problem ($\Phi_p^- \neq 0$), Eqs. (6, 5b, and 7) deliver $\Phi_Y^+(X,0) = [\Phi_p^+(X,0)]_Y$ and $\Phi_X^- = \Phi_Y^- = 0$. On the other hand, from $\Phi_p^+ \equiv 0$ follows $\Phi_Y^- \neq 0$ and $\Phi_Y^+ = 0$. Consequently, there is no analogous purely antisymmetric case.

Integrating Eq. (5a) by parts, and taking the value on the body axis using the principal value definition of Oswatitsch,[1] there follows the integral equation of the present problem

$$u^+(X,0) = U_p^+(X,0) + \frac{[u^+(X,0)]^2}{2} + U_A(X,0)$$

$$- \frac{1}{2\pi}\int_{-\infty}^{\infty}\int_{-\infty}^{\infty} \frac{[U^+(\xi,\eta)]^2}{2} \times \frac{(X-\xi)^2 - \eta^2}{[(X-\xi)^2+\eta^2]^2}\, d\xi d\eta \quad (8)$$

where

$$U_A(X,0) = \frac{[U_p^-(X,0)]^2}{2} - \frac{1}{2\pi}\int_{-\infty}^{\infty}\int_{-\infty}^{\infty} \frac{[u_p^-(\xi,\eta)]^2}{2} \times \frac{(X-\xi)^2-\eta^2}{[(X-\xi)^2+\eta^2]^2}\, d\xi d\eta \quad (9)$$

corresponds to the antisymmetric part of Eq. (5a) and is a known quantity.

The boundary conditions[1,2] are

$$U = 0 = V, \text{ as } (X^2+Y^2)^{1/2} \to \infty \quad (10a)$$

and

$$[V(X,Y)]_{\text{profile}} = \frac{1}{(1-M_\infty^2)^{1/2}(1/M_\infty^* - 1)}$$

$$\times\left[\pm g'(x) + f'(x) - \frac{v_\infty}{u_\infty}\right] \approx V(X, \pm 0) \quad (10b)$$

where M_∞ denotes freestream Mach number and the superscript "*" represents its critical value, $g(x)$ and $f(x)$ give the thickness and camber distribution of the profile, and v_∞ and u_∞, the freestream velocity components.

To find an approximate solution of the nonlinear, two-dimensional singular integral equation (8), where $U_p^+(X,0)$ and $U_A(X,0)$ are known functions, the following inversion formula proved in Ref. 8 is used for the parameter value $a = 1$, which is a good choice as evident from previous computations including that for Nieuwland profiles.

If $g(x,y)$ be a known function, square integrable in Lebesgue sense in Euclidean space E_2, then the unique exact solution of the two-dimensional integral equation

$$Q(X,Y) - \frac{1}{2\pi}\int_{-\infty}^{\infty}\int_{-\infty}^{\infty} Q(\xi,\eta) \frac{(\xi-x)^2-(\eta-Y)^2}{[(\xi-X)^2+(\eta-Y)^2]^2}\, d\xi d\eta = g(X,Y)$$

is

$$Q(X,Y) = \frac{2}{(3)^{1/2}} g(X,Y)$$

$$+ \frac{2}{\pi(3)^{1/2}}\int_{-\infty}^{\infty}\int_{-\infty}^{\infty} g(\xi,\eta) \frac{(\xi-X)^2 - 3(\eta-Y)^2}{[(\xi-X)^2+3(\eta-Y)^2]^2}\, d\xi d\eta \quad (11)$$

In these integrals, the kernels are singular at $\xi = X$, $\eta = Y$, where a principal value definition is used indicated by the symbol "⊙" beneath the double integral, according to which the singularity is removed by drawing a small circle around it and taking the limit as the radius approaches zero. To apply the inversion formula, Eq. (11), the integral equation (8) is rewritten in the form

$$U^+(X,0) = [U_p^+(X,0) + U_A(X,0)] + \frac{[U^+(X,0)]^2}{4}$$

$$- \frac{1}{2\pi}\int_{-\infty}^{\infty}\int_{-\infty}^{\infty} \frac{[U^+(\xi,\eta)]^2}{2} \frac{(\xi-X)^2-\eta^2}{[(\xi-x)^2+\eta^2]^2}\, d\xi d\eta$$

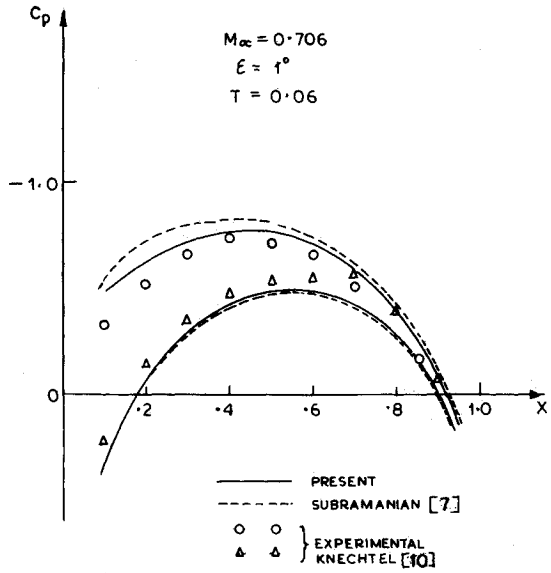

Fig. 1 Reduced pressure coefficient on symmetric parabolic arc profile at incidence.

which is then put to the form

$$[U^+(X,0)]^2 - \frac{1}{2\pi}\int_{-\infty}^{\infty}\int_{-\infty}^{\infty}[U^+(\xi,\eta)]^2 \times \frac{(\xi-X)^2-\eta^2}{[(\xi-X)^2+\eta^2]^2}\,d\xi d\eta = [2U^+(X,0) - 2U_p^+(X,0) - 2U_A(X,0) + 1/2[U^+(X,0)]^2] \quad (12)$$

Now applying the inversion formula of Eq. (11) to Eq. (12), we get

$$[U^+(X,0)]^2 = 2/(3)^{1/2}[2U^+(X,0) - 2U_p^+(X,0) - 2U_A(X,0) + \tfrac{1}{2}[U^+(X,0)]^2] + 2/(3)^{1/2}I(X,0) \quad (13)$$

where

$$I(X,0) = \frac{1}{\pi}\int_{-\infty}^{\infty}\int_{-\infty}^{\infty}[3U^+(\xi,\eta) - 2U_p^+(\xi,\eta) - 2U_A(\xi,\eta)]\,\frac{(\xi-X)^2-3\eta^2}{[(\xi-X)^2+3\eta^2]^2}\,d\xi d\eta - \frac{1}{\pi}\int_{-\infty}^{\infty}\int_{-\infty}^{\infty}\left[U^+(\xi,\eta) - \frac{[U^+(\xi,\eta)]^2}{2}\right] \times \frac{(\xi-X)^2-3\eta^2}{[(\xi-X)^2+3\eta^2]^2}\,d\xi d\eta \quad (14)$$

This kernel has the property that when multiplied by a constant or by U_p^+, its integral over whole space vanishes identically. Moreover, the integrals are not sensitive to small changes in the value of $U^+(\xi,\eta)$. Consequently, we may take $U_p^+(\xi,\eta)$ as a first approximation of $U^+(\xi,\eta)$ in the first integral of Eq. (14). In general, the value of U_A is small compared to U_p^+, which is about 2-3% for the examples presented here. Further, its values remain more or less constant throughout the interval. Hence, as an approximation, it leads to a zero value of the integral. Moreover, in the second integral the factor in the square bracket represents the mass flux density in the transonic speed range and it does not exceed the value 1/2, so that the second integral is also small, particularly in the region where the local Mach number is near the critical Mach number. Thus, neglecting $I(X,0)$ in comparison with $U_p^+(X,0)$, solving the quadratic expression, Eq. (13), and using Eq. (6), we get an approximate solution

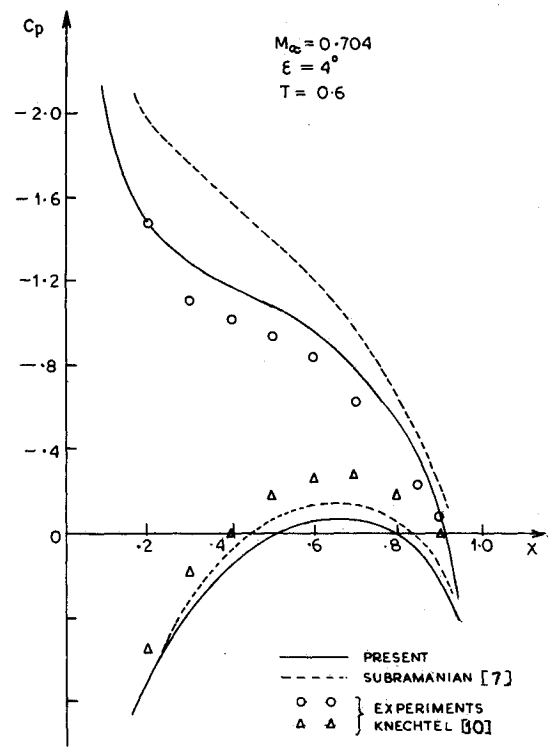

Fig. 2 Reduced pressure coefficient on symmetric parabolic arc profile at incidence.

$$U(X,0) = U^+(X,0) + U^-(X,0) = [(3)^{1/2}+1]\,[1-(1-[(3)^{1/2}-1][U_p^+(X,0)+U_A(X,0)])^{1/2}] + U_p^-(X,0) \quad (15)$$

on the upper surface and

$$U(X,0) = U^+(X,0) - U^-(X,0) \quad (16)$$

on the lower surface of the profile where the symmetric and antisymmetric part of the linearized solution $U_p(X,0)$ at an angle of attack ϵ is given by[1]

$$U_p^+(X,0) = \frac{1}{\pi}\int_0^1 \tfrac{1}{2}[V_u(\xi) - V_l(\xi)]\,\frac{d\xi}{X-\xi} \quad (17)$$

and

$$U_p^-(X,0) = \frac{1}{\pi}\,\frac{1}{[X(1-X)]^{1/2}} \int_0^1 \tfrac{1}{2}[V_u(\xi)+V_l(\xi)]\,[\xi(1-\xi)]^{1/2} \times \left[\frac{1}{X-\xi} - \frac{1}{1-\xi}\right]d\xi + \epsilon'\left(\frac{1-X}{X}\right)^{1/2} \quad (18)$$

Here ϵ' is the reduced angle of attack given by

$$\epsilon' = \epsilon/[(1/M_\infty^* - 1)\,(1-M_\infty^2)^{1/2}] \quad (19)$$

and the velocity components along X axis on the upper and lower surface $V_u(\xi)$ and $V_l(\xi)$ can be determined from the boundary conditions.

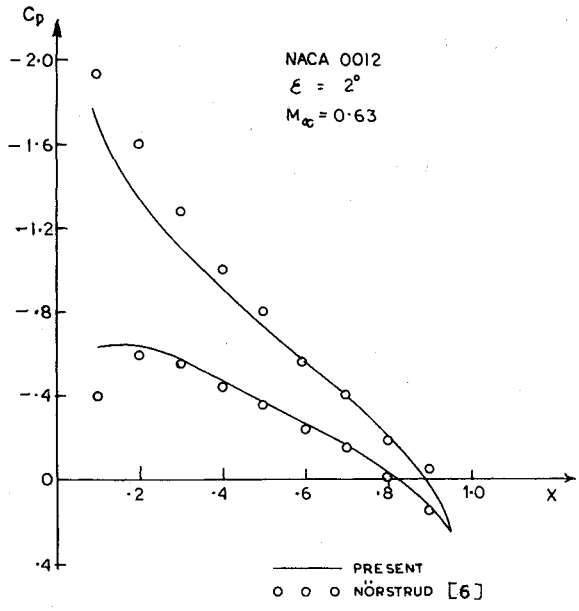

Fig. 3 Reduced pressure coefficient at NACA 0012 profile at incidence.

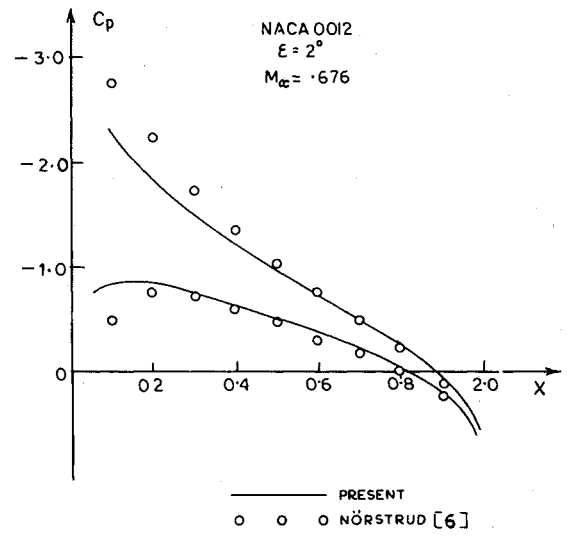

Fig. 4 Reduced pressure coefficient at NACA 0012 profile at non-zero incidence.

For evaluating the solution, Eq. (15), it is necessary to compute the integral part of U_A given by Eq. (9), which contains a double integral over the known function U_p^-. To find an approximate value of the double integral we make the substitution

$$U_p^-(X,Y) = U_p^-(X,0)\ [1+Y/b(X)]^{-2} \qquad (20)$$

where $b(x)$ is an unknown parameter to be determined by the irrotationality condition. A similar substitution has been previously used by many authors[2] and is known to be a good one. Substituting Eq. (20) in Eq. (9), carrying out the indicated integration with respect to η, and noting the observations made therein[2] we get

$$U_A = (U_p^-)^2/2 - \int_0^1 \frac{[U_p^-(\xi,0)]^2}{2\,b(\xi)} \cdot E\left(\frac{\xi - x}{b}\right) d\xi \qquad (21)$$

where

$$E(x) = \frac{4}{\pi}\,\frac{1}{(1+X^2)^5}\left[\frac{\pi}{2}(5-10X^2+X^4)\,|X| - (1-10X^2+5X^4)\ln|X| - \frac{1}{12}(25-71X^2-X^4-X^6)(1+X^2)\right] \qquad (22)$$

For performing the integration in Eq. (21), Simpson's one third rule has been used, the singularities at $\xi = X, 0$, and 1 appropriately being taken care of.

The reduced pressure coefficient $C_p = -2U(X,0)$ for a parabolic arc profile at small incidence has been computed by the preceding method and compared with theoretical results[7] and with the experimental results of Knechtel[10] in Figs. 1 and 2, respectively, for subcritical and supercritical flow. From the figures, it is apparent that the present solution agree well with the experimental results. It should be mentioned that the agreement of the present solution with the experimental results of Knechtel for a parabolic arc profile at an incidence of 4° is particularly noteworthy (Fig. 2). The reduced pressure coefficients for NACA 0012 profile for different freestream Mach number M_∞ and angle of incidence ϵ have been presented in Figs. 3 and 4, where Fig. 4 shows a supercritical finite difference solution of the integral equation by Nörstrud.[6] The agreements are excellent. Thus it appears that the present solution is capable of delivering satisfactory results at a very low expenditure of labor. To compute one example of a lifting profile by this method takes only 5 minutes on an IBM 1130 electronic digital computer.

References

[1] Oswatitsch, K., *Gas Dynamics*, Chap. 9, Academic Press, New York, 1956.

[2] Ferrari, C. and Tricomi, F. G., *Transonic Aerodynamics*, Chap. 6, Academic Press, New York, 1968.

[3] Oswatitsch, K., ed., *Symposium Transonicum*, Springer-Verlag, West Berlin, 1964.

[4] Nieuwland, G. Y., "Transonic Potential Flow around a Family of Quasielliptical Aerofoil Sections," Rept. TR T172, 1967, NLR, The Netherlands.

[5] Holder, D. W., "Transonic Flow Past Two Dimensional Aerofoils," *Journal of the Royal Aeronautical Society*, Vol. 68, 1964, pp. 501-516.

[6] Nörstrud, H., "Transonic Aerofoil Problems with Embedded Shocks," *Aeronautical Quarterly*, May 1973, pp. 129-138.

[7] Subramanian, N. R. Balakrisnan, M., "Transonic Flow Past Lifting Airfoils," *AIAA Journal*, Vol. 11, Dec. 1973, pp. 1766-1768.

[8] Niyogi, P. and Mitra, R., "Approximate Shock-Free Transonic Solution for a Symmetric Profile at Zero Incidence," *AIAA Journal*, Vol. 11, April 1973, pp. 751-754.

[9] Nörstrud, H., "Numerische Lösungen für Schallnahe Strömungen um Ebene Profile," *Zeitschrift für Flugwissenschaften*, Vol. 18, 1970, pp. 149-157.

[10] Knechtel, E. D., "Experimental Investigation at Transonic Speeds of Pressure Distribution over Wedge and Circular Arc Airfoil Sections and Evaluation of Perforated Wall Interference," TN D-15, 1959, NASA.

Mean-Square Response of Beams to Nonstationary Random Excitation

G. Ahmadi* and M.A. Satter*
Pahlavi University, Shiraz, Iran

Introduction

VIBRATION of elastic structures to random loads is of considerable interest to the design engineer. The early study of the response of beams and plates to random ex-

Received September 20, 1974. The authors would like to thank the Research Council of the Ministry of Higher Education of Iran for their financial support through Grant 870-102-870-1-52.

Index categories: VTOL Vibration; LV/M Structural Design (including Loads); Structural Dynamic Analysis.

*Associate Professor, Department of Mechanical Engineering.